

Received October 25, 2019, accepted November 9, 2019, date of publication November 12, 2019, date of current version November 25, 2019.

Digital Object Identifier 10.1109/ACCESS.2019.2953040

A Novel Model for Sex Discrimination of Silkworm Pupae From Different Species

DAN TAO¹, GUANGYING QIU², AND GUANGLIN LI³

¹College of Electrical and Automation Engineering, East China Jiaotong University, Nanchang 330013, China

²Rail Transportation Technology Innovation Center, East China Jiaotong University, Nanchang 330013, China

³College of Engineering and Technology, Southwest University, Chongqing 400716, China

Corresponding authors: Guangying Qiu (qiuguangying602@163.com) and Guanglin Li (guanglinli_email@163.com)

This work was supported in part by the Chongqing Science and Technology Commission Project under Grant cstc2017shms-xdny80080, and in part by the National Natural Science Foundation of China under Grant 31971782.

ABSTRACT Sex determination of silkworm pupae is important for silkworm industry. Multivariate analysis methods have been widely applied in hyperspectral imaging spectroscopy for classification. However, these methods require essential steps containing spectra preprocessing or feature extraction, which were not easy determined. Convolutional neural networks (CNNs), which have been employed in image recognition, could effectively learn interpretable presentations of the sample without the need of ad-hoc preprocessing steps. The species of silkworm pupae are usually up to hundreds. Conventional classifiers based on one species of silkworm pupae could not give high performance when explored to other species that not participating in the model building, resulting in bad generalization ability. In this study, a CNN model was trained to automatically identify the sex of silkworm pupae from different years and species based on the hyperspectral spectra. The results were compared with the frequently used conventional machine classifiers including support vector machine (SVM) and K nearest neighbors (KNN). The results showed that CNN outperformed SVM and KNN in terms of accuracy when applied to the raw spectra with 98.03%. However, the performance of CNN decreased to 95.09% when combined with the preprocessed data. Then principal component analysis (PCA) was adopted to reduce data dimensionality and extract features. CNN gave higher accuracy than SVM and KNN based on PCA. The discussion section revealed that CNN had high generalization ability that could classify silkworm pupae from different species with a rather well performance. It demonstrated that HSI technology in combination with CNN was useful in determining the sex of silkworm pupae.

INDEX TERMS Silkworm pupae, sex, hyperspectral imaging, convolutional neural network.

I. INTRODUCTION

China has a long history in silk production and exportation. Before crossbreeding, it is necessary to determine the sex of silkworm pupae that finished manually. There have several researches for automatically identifying the sex of silkworm pupae [1]–[7]. Among these methods, the spectroscopy technology is promising because of its high accuracy and effectiveness. Designing a classification model based on spectroscopy technology to determine the sex of silkworm pupae of different species and seasons is challenging, because the generalization ability of conventional classifiers that including support vector machine (SVM), partial least squares discriminant analysis (PLS-DA), linear discriminant analysis (LDA), artificial neural networks (ANN) is not good.

The associate editor coordinating the review of this manuscript and approving it for publication was Yudong Zhang.

Hence, it is important to build a classification model to classify the sex of silkworm pupae with high performance.

Nowadays, Hyperspectral imaging (HSI) technology has become a widespread method that simultaneously contains the spectral and spatial data. Many studies have reported about employing HSI technology to do the classification work [8]–[10]. We have explored the HSI technology to discriminate the sex of silkworm pupae by combing the textural characteristics and spectra features [11]. The model reaches high accuracy. However, the generalization ability of the conventional classifiers is not well. Currently, chemometrics research mainly focuses on the problem of selecting a useful preprocessing method and feature extraction method. It cannot be ignored that the selected methods may work well for one dataset, but do not work when applied to another dataset collected using a different sample matrix or experiment setting.

The performance for the hyperspectral spectra strongly depends on the training set employed in the modeling process. If the samples in the model are not representative, the classification results are bad [12]. About the maize seed classification based on HSI, when the model was explored to classify the seeds from the next year, the performance decreased because new variances were introduced by changes in cultivation conditions from one year to another. Guo *et al.* [12], Zhang [13] and Huang *et al.* [14] updated the classification model to classify the seeds from the next year. For silkworm pupae samples, the species are up to hundreds. Previous studies only use the model to differentiate the sex of silkworm pupae from the current year and the same species. No studies have ever explored the performance of the developed model to discriminate the silkworm pupae from the next year. Hence, it is necessary to design a classification model based on HSI that could differentiate the silkworm pupae from different species and years with high performance.

Convolutional Neural Networks (CNNs), as one of the most popular deep learning models, first presented by Lecun *et al.* [15] in 1998, has been widely exported in image classification and has high classification performance and generalization ability [16], [17]. CNNs are nonlinear classifiers that can identify the unseen samples without the need for feature extraction. CNNs have been applied for classification of two-dimensional image and three-dimensional hyperspectral remote sensing data [18]. To the best of our knowledge, unlike the conventional spectra analysis pipelines, CNN combines preprocessing, feature extraction and classification in a single architecture that is trained end-to-end without manual tuning. The work developed by Acquarelli *et al.* [19] and Liu *et al.* [20] are the only places where CNN is used over 1-dimensional (1D) input signals. Therefore, CNN model could effectively to determine sex of silkworm pupa from different species and years.

In this work, a new CNN model is developed in the context of sex determination of silkworm pupae of different species based on HSI spectra. The objectives were: (1) to develop a CNN model; (2) to compare the performance of CNN with SVM and KNN on the raw spectra with or without preprocessing; (3) to compare the classification ability of CNN with SVM and KNN on the test set from different species and the next year.

II. MATERIALS AND METHODS

CNNs are designed to extract the features from an input signal. A typical CNN includes convolutional layers and pooling operators that effectively extract the features hierarchically. Features determined by network training are optimal in the sense of the performance of the classifier. The end-to-end trainable systems of CNN offer a much better alternative to a pipeline in which each part is trained independently or crafted manually.

A. CNN MODEL TRAINED FOR SEX CLASSIFICATION

The input full spectra of silkworm pupae to CNN are one dimension. Accordingly, we train the one-dimensional

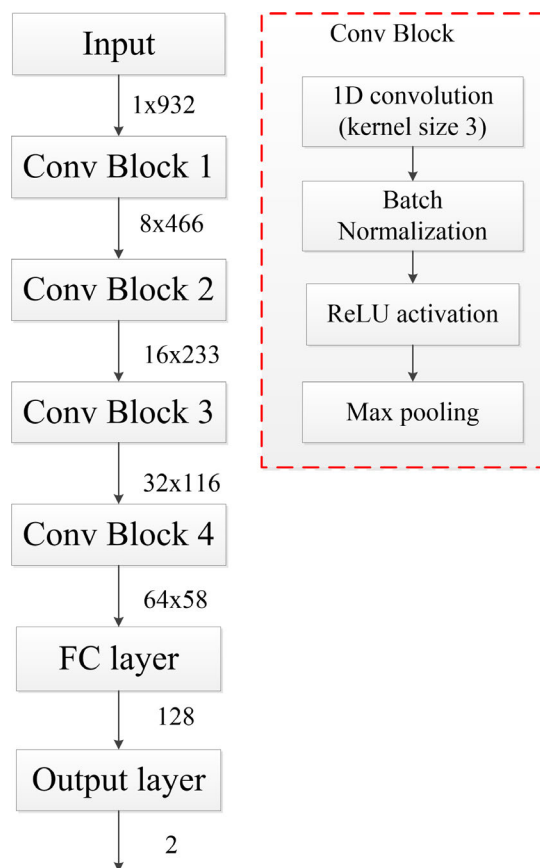


FIGURE 1. The general architecture of 1D-CNN.

convolutional kernels in CNN, as shown in Figure 1. In Figure.1, an example of 932 spectral bands was applied to display the output size of each block. There are four main blocks in the architecture. The first four blocks are convolutional blocks, each of which consists of a convolutional layer, Batch normalization layer, ReLU activation function and a max pooling layer. As convolution blocks going deeper, the number of filters is doubled (starting from 8 to 64). All convolutional layers adopt a kernel size of 3, stride of 1 and padding of 1. A convolutional layer has local connections to its input and can be trained to learn local patterns. By chaining convolutional layers together, deeper layers have connection to large part of the raw input. Accordingly, different layers acquire the raw input and learn features at different levels. The last block is fully connected layer, which is applied to learn combinations of features extracted by the convolutional layers. Finally, an output layer includes a softmax layer and a classification layer (2 classes, female and male). We will present the design of each part of CNN architecture in the following sections in details.

B. CONVOLUTION LAYER

In the convolution layer, convolutions are performed between the previous layer and a series of filters, which are employed to extract features from the previous layer. Then, the outputs

of the convolutions will add an additive bias and an element-wise non-linear activation function is applied on the results. Here, it usually adopts the ReLU function as the nonlinear function. The expression of convolution is shown as follows,

$$y^j = f \left(\sum_i x^i * k^{ij} + b^j \right) \quad (1)$$

where y^j is the j -th output map and x^j denotes the j -th input map, k^{ij} is the convolution kernel, b^j is the offset parameter, $*$ denotes convolution, and $f(\cdot)$ is the nonlinear active function. However, the sigmoid function easily leads to saturated, which affects the convergence rate of the net in the deep network. Hence, it usually adopts the ReLU function as the nonlinear function in the deep network, and the expression of ReLU function is shown as follows,

$$\text{ReLU}(x) = \begin{cases} x & x \geq 0 \\ 0 & x < 0 \end{cases} \quad (2)$$

d^l and r^l are supposed to the dimension of the final output of each feature signal on the layer l and the length of its corresponding kernel. The final output of the feature signal of the next layer $l + 1$ is shown in below,

$$d^{l+1} = \frac{d^l - r^l + 1}{2} \quad (3)$$

The upper layers of CNN are fully connected and followed by the softmax with the number of outputs that is equals to the number of classes. The softmax function is expressed as follows,

$$p(z)_w = \frac{e^{z_w}}{\sum_{k=1}^K e^{z_k}} \quad w = 1, \dots, K \quad (4)$$

where z denotes the output of CNN, w represents a class and K is the total number of classes.

The one-dimensional kernel was adopted because each spectrum was expressed as a one-dimensional array. After the convolutional layer, a fully connected output layer with the number of units equaled to the number of classes was employed. The use of the softmax activation function on this output layer allowed obtaining the class results of the network in response of an input sample.

C. TRAINING PARAMETERS OF PROPOSED MODEL

For the training of the designed CNN model, Stochastic Gradient Descent with Momentum (SGDM) updating rule was adopted. It could effectively overcome the instability of Stochastic Gradient Descent (SGD) to some extent, improving the learning rate and solving the local optimum. In general, the training parameters were chosen as follows. The epochs was set to 100, mini-batch size as 8, the initial learning rate as 0.001. The momentum determines the contribution of the gradient step from the previous iteration to the current iteration of training, which is usually set to be 0.9 [21], [22].

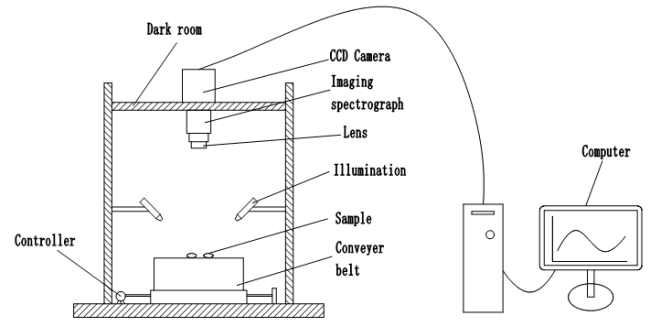


FIGURE 2. Schematic diagram of hyperspectral imaging system.

III. SAMPLE ACQUIRING

As Table 1 depicted, 2862 silkworm pupae were used in the experiment. Those samples were acquired in two seasons and consisted of four hybrid species. The sex ratio of all silkworm pupae was close to 1:1. A total of 707 (24.70%) samples of 871A \times 447 species and 664 (23.20%) of 872B \times 953 were acquired in June 2017. A total of 749 (25.93%) samples of Su \times 471 and 749 (26.17%) samples of Ming \times 970 were bought in June 2018. The diversity of samples could effectively increase the generalization ability of the developed model in a large extent.

A. HYPERSPECTRAL DATA CORRECTION AND PREPROCESSING

Data were acquired using the laboratory-based HSI system (363-1026nm) mainly containing spectrograph (ImSpector V10E, Spectral Imaging Ltd., Oulu, Finland), EMCCD (Raptor EM285CL, China), two fiber halogen lamps (IT 3900, 150W), a computer with data acquisition and pre-processing software (Spectral Image software, Isuze Optics Corp., Taiwan, China), as shown in Fig. 2. The HSI system was preheated about one hour before software collecting data. The spectral resolution was 0.5nm. The distance between the lens and the samples was set to 20cm, and the movement speed of platform was set to 0.85mm/s.

The exposure time was set to 21ms. The resolution of the raw image was 1632 \times 1232 (spatial \times spectral) pixels. The processing software includes ENVI 4.6 (ITT Visual Information Solutions, Boulder, Utah, USA) and Matlab 2017b (The Math Works, Natick, MA, USA). Then the HSI data were corrected by minimizing the differences among samples caused by sensor response and illumination. The mean spectra were extracted from the region of interest (ROI). To avoid noise at the beginning bands and the ending bands due to the limitation of the hyperspectral imaging system, the spectra ranging in 400-900nm were selected. Then, standard normal variate (SNV) was employed to remove the data artifacts and scattering effects here.

B. RAW HSI DATA PROCESSING STEPS

The raw HSI data processing steps were shown in Fig. 3. Firstly, the raw HSI data were corrected by minimizing the differences among samples caused by sensor response and

TABLE 1. Statistics results for the sets of silkworm pupae.

Data of experiment	Hybrid varieties	Number of Females	Number of Males	Total (%)
June 2017	871A×447	399	308	707 (24.70)
June 2017	872B×953	304	360	664 (23.20)
June 2018	Su×471	355	387	742 (25.93)
June 2018	Ming×970	370	379	749 (26.17)
Total (%)		1428 (49.89)	1434 (50.11)	2862 (100)

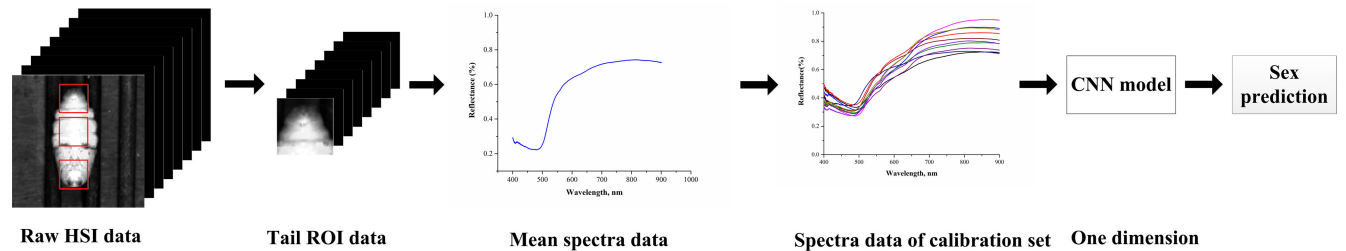


FIGURE 3. The flowchart of raw HSI data processing steps.

illumination. Then, the tail region of interest (ROI) was chosen, which was detailed discussed in the part 3.2.1 “The selection of ROI” in our previous work [11]. Then, the mean spectra were computed to represent the tail ROI data. The spectra data of calibration set contained the spectra of multiple tail ROI data. To avoid noise at the beginning bands and the ending bands due to bands due to the limitation of the hyperspectral imaging system, the spectra ranging in 400-900nm were selected. Finally, the one dimension CNN model was built based on the spectra of calibration set, which could be used to predict the sex of silkworm pupae in the testing set.

C. OTHER CLASSIFICATION METHODS

1) SUPPORT VECTOR MACHINE

As an effective analysis tool, SVM has been widely applied in many fields. Its theory for the classification and regression has been described in detail [23], [24]. The main thought of SVM is to represent the original category of the sample in a higher space, which is called feature space. A complex non-linear mapping of variables to feature space can be realized by SVM. The variables are expressed in the feature space and are distinguished more easily than those in the original space [25], [26]. It has been shown that radial basis function (RBF) is more effective than other kernel functions [27]. RBF is described as Eq.5,

$$M(x, x_t) = \exp\left(-\frac{\|x - x_t\|^2}{2g^2}\right) \quad (5)$$

where $\|x - x_t\|$ calculates the distance from the t -th input vector and the threshold vector, g represents the width parameter. The parameter c and g are usually searched grid-search procedure.

2) K NEAREST NEIGHBORS

K nearest neighbor (KNN), as a type of pattern recognition method, calculates the distances between an unknown sample

and the samples in the training set [28]. The number of nearest samples (k) to the unknown sample is determined by the categories manually specified. The category of the unknown sample is of its k nearest samples in the training set. The determination of k is crucial for KNN, which is optimized by comparing KNN models using different k . We consider a number of neighbors of $k \in [3, 10]$.

3) ASSESSMENT METRICS

Four parameters including precision, recall, F measure and accuracy are computed as the index to access the performance of model. Precision represents the ability of classifier to label a positive sample that is positive. The F measure is harmonic mean of precision and recall. Accuracy is the total recognition rate of classifier [29].

$$Precision = \frac{TP}{TP + FP} \quad (6)$$

$$Recall = \frac{TP}{TP + FN} \quad (7)$$

$$F = \frac{2 * precision * recall}{precision + recall} \quad (8)$$

$$Accuracy = \frac{TP + TN}{TP + FN + FP + TN} \quad (9)$$

True positive (TP) and true negative (TN) respectively represent the positive samples and negatives samples that are correctly classified. False positive (FP) denotes the negative samples that are incorrectly as positive. False negative (FN) refers to the samples that are misclassified as negative.

IV. RESULTS AND DISCUSSION

Fig.4 depicted the average reflectance spectra characteristics of silkworm pupae with or without preprocessing. In Fig.4(a), the general trend of mean female curve and male curve was similar. In Fig.4, an obvious absorption peak could be

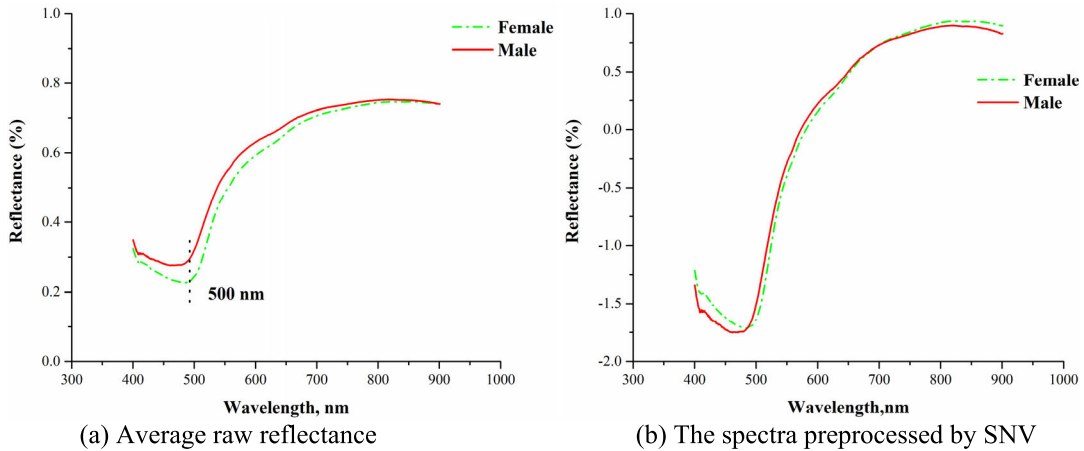


FIGURE 4. Spectra curves of silkworm pupae.

TABLE 2. Silkworm pupae samples from different species.

Data set	871A×447		872B×953		Su×471		Ming×970		Total
	Female	Male	Female	Male	Female	Male	Female	Male	
Calibration set	299	232	228	270	266	290	278	285	2148
Testing set	100	76	76	90	89	97	92	94	714

TABLE 3. Classification accuracy of classifiers on raw data with or without preprocessing.

Data	Classifiers	Discriminated sex				Precision	Recall	F measure	accuracy
		NFM (357)		NM (357)					
		FM	M	FM	M				
Raw	SVM	280	77	87	270	76.29	78.43	77.35	77.03
	KNN	274	83	95	262	74.25	76.75	75.48	75.07
	CNN	348	9	5	352	98.58	97.48	98.03	98.03
Pretreating	SVM	319	38	40	317	88.85	89.36	89.10	89.11
	KNN	305	52	55	302	84.72	85.43	85.07	85.01
	CNN	343	14	21	336	94.23	96.08	95.15	95.09

observed near 500nm. The spectra preprocessed with Standard normal variate (SNV) were shown in Fig.4.(b). These differences were the basis for using the hyperspectral imaging to the sex determination of silkworm pupae.

A. CLASSIFICATION RESULTS

Before constructing the classification model, female and male silkworm pupae from different species were divided into a calibration set and a test set according to the ratio of 3:1 using Kennard stone (KS) algorithm, as shown in Table 2.

1) CLASSIFICATION RESULTS USING PREPROCESSING

The sex discrimination results on the raw data with or without preprocessing were shown in Table 3. A good model should have high accuracy, sensitivity, specificity and precision. In Table 3, it showed that CNN model reached significantly best performance based on the raw data with accuracy of 98.03%, precision 98.58%, recall 97.48% and F score 98.03%. After preprocessed with SNV, the accuracy of CNN

decreased to 95.09%, while the accuracy of SVM and KNN was improved to 89.11% and 85.01%, respectively.

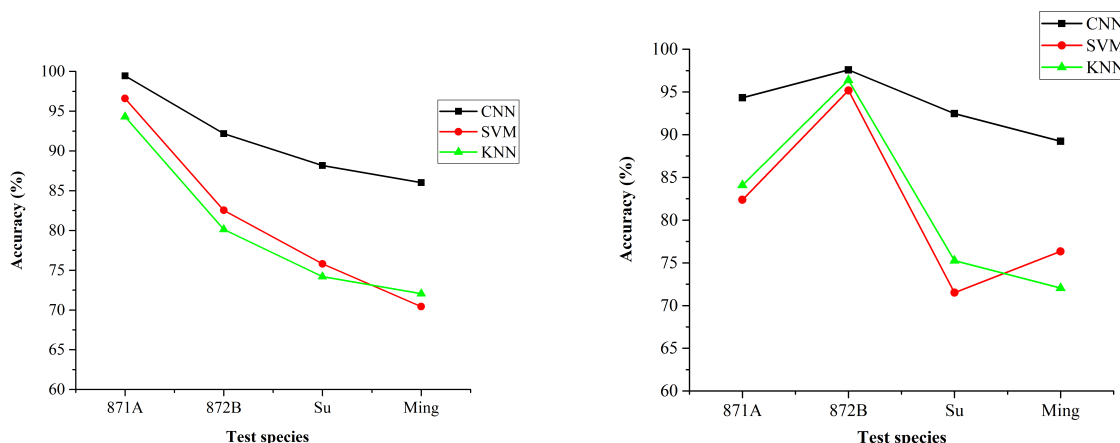
It was not surprised that convolutional classifiers (SVM, KNN) were usually not able to cope with the spectra that were not well pretreated, and therefore need explicit pretreating methods in the processing pipeline. On the other hand, CNN could intelligently handle the interference of the baselines.

2) IDENTIFICATION RESULTS USING PCA

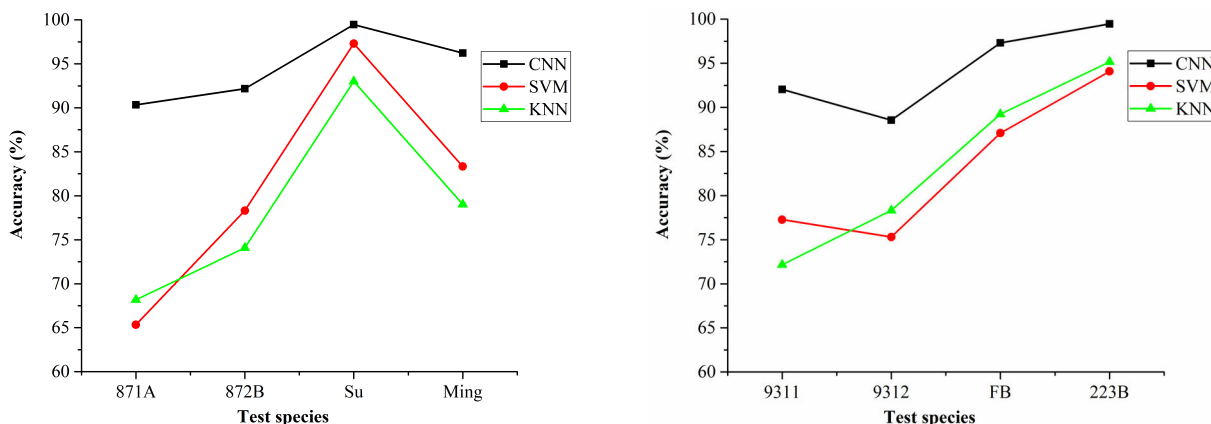
After the raw spectra pretreated, PCA was applied to reduce the data dimensionality. The number of principal components was selected such that 99.9% of total variance was retained. The results were depicted in Table 4. In Table 4, CNN gave the highest performance based on PCA with precision 96.93%, recall 97.20%, F measure 97.06% and accuracy 97.06%. Compared with results without PCA in Table 3, SVM and KNN performed better, while the performance of CNN decreased. It revealed that PCA had the ability to extract discriminated features from the spectra of female

TABLE 4. Classification accuracy of classifiers on raw data with or without preprocessing.

Classifiers	Discriminated sex				Precision	Recall	F measure	Accuracy
	NFM(357)		NM(357)					
	FM	M	FM	M				
SVM	346	11	17	340	95.32	96.92	96.11	96.07
KNN	343	14	21	336	94.23	96.07	95.14	95.09
CNN	347	10	11	346	96.93	97.20	97.06	97.06



(a) The identification model built based on 871A×447 species in June 2017 (b) The identification model built based on 872B×953 species in June 2017



(c) The identification model built based on Su×471 species in June 2018 (d) The identification model built based on Ming×970 species in June 2018.

FIGURE 5. The classification results on silkworm pupae from different species.

and male silkworm pupae. Besides, CNN model could reach high performance of classification while requiring minimal preprocessing of spectra.

3) DISCUSSION

The species of silkworm pupae is up to hundreds. The sex discrimination model built using one species needs to rebuild when applied to another species. However, it is time-consuming to rebuild model in the online discrimination system. Accordingly, it is necessary to design a new model. As we known, CNN has quite good generalization ability. To further substantiate this characteristic of CNN,

the calibration set of each species were applied to build model and then the model was used to differentiate the test set of the remaining species. The results were shown in Table 5. The details were drawn in Fig. 5. The calibration set of 871A × 447, 872B × 953, Su × 471, Min × 970 was applied to build the model, as shown in Fig.5a, Fig.5b, Fig.5c, Fig.5d, respectively. As Fig.5 shown, CNN performed better than SVM and KNN when the model was adopted to classify the test set, indicating that CNN had better generalization ability.

Two points were highlighted by observing four figures. Firstly, the accuracy of the model was the highest when

TABLE 5. Classification accuracy of classifiers on raw data with or without preprocessing.

Classifier	Season	Calibration set (number)	Accuracy			
			871A×447 (176)	872B×953 (166)	Su×471 (186)	Ming×970 (186)
SVM	June 2017	871A×447 (531)	96.59	82.53	75.80	70.43
SVM	June 2017	872B×953 (498)	82.38	95.18	71.51	76.34
SVM	June 2018	Su×471 (556)	65.34	78.31	97.31	83.33
SVM	June 2018	Min×970 (563)	77.27	75.30	87.09	94.08
KNN	June 2017	871A×447 (531)	94.31	80.12	74.19	72.04
KNN	June 2017	872B×953 (498)	84.09	96.38	75.26	72.04
KNN	June 2018	Su×471 (556)	68.18	74.09	93.01	79.03
KNN	June 2018	Min×970 (563)	72.16	78.31	89.24	95.16
CNN	June 2017	871A×447 (531)	99.43	92.17	88.17	86.02
CNN	June 2017	872B×953 (498)	94.32	97.59	92.47	89.24
CNN	June 2018	Su×471 (556)	90.34	92.17	99.46	96.23
CNN	June 2018	Min×970 (563)	92.04	88.55	97.31	99.46

the calibration set and test set were from the same species. Secondly, when the built model was applied to classify the silkworm pupae from different species, the species from the same year with the built model achieved higher accuracy than that from the different year. The reason may be that with feeding environment and climate changing from year to year, silkworm pupae had many differences.

Compared the prediction accuracy of sex classification of silkworm pupae with other research, this paper gave almost the same performance when the calibration set and testing set from the same species and years. However, when the built model was promoted to classify silkworm pupae from different species, the CNN model with high generalization ability proposed in this paper, outperformed other studies.

V. CONCLUSION

In this paper, we proposed a CNN model for sex classification of silkworm pupae based on HSI spectra with high performance. The CNN model outperformed other state-of-the-art machine learning methods (SVM, KNN) using the raw spectra or the spectra processed with pretreating and PCA. Results indicate that CNN is less dependent on preprocessing and feature extraction compared to SVM and KNN. This study will make contributions to the online intelligent sex recognition of silkworm pupae.

CONFLICT OF INTEREST

The authors declare that there are no conflicts of interest regarding the publication of this paper.

REFERENCES

- [1] Y. Seo, H. Morishima, and A. Hosokawa, "Separation of male and female silkworm pupae by weight: Prediction of separability," *Jpn. Soc. Agricult. Mach.*, vol. 47, no. 2, pp. 191–195, 1985.
- [2] Z. Zhu, H. Yuan, C. Song, X. Li, D. Fang, Z. Guo, X. Zhu, W. Liu, and G. Yan, "High-speed sex identification and sorting of living silkworm pupae using near-infrared spectroscopy combined with chemometrics," *Sens. Actuators B, Chem.*, vol. 268, pp. 299–309, Sep. 2018.
- [3] J.-R. Cai, L.-M. Yuan, B. Liu, and L. Sun, "Nondestructive gender identification of silkworm cocoons using X-ray imaging with multivariate data analysis," *Anal. Methods*, vol. 6, no. 18, pp. 7224–7233, 2014.
- [4] C. Liu, Z. H. Ren, H. Z. Wang, P. Q. Yang, and X. L. Zhang, "Analysis on gender of silkworms by MRI technology," in *Proc. Int. Conf. BioMed. Eng. Inform.*, vol. 2, pp. 8–12, May 2008.
- [5] C. Kamtongdee, S. Sumriddetchkajorn, and C. Sa-Ngiamsak, "Feasibility Study of silkworm pupa sex identification with pattern matching," *Comput. Electron. Agricult.*, vol. 95, pp. 31–37, Jul. 2013.
- [6] S. Sumriddetchkajorn, C. Kamtongdee, and S. Chanhorm, "Fault-tolerant optical-penetration-based silkworm gender identification," *Comput. Electron. Agricult.*, vol. 119, pp. 201–208, Nov. 2015.
- [7] D. Tao, Z. Wang, G. Li, and G. Qiu, "Accurate identification of the sex and species of silkworm pupae using near infrared spectroscopy," *J. Appl. Spectrosc.*, vol. 85, no. 5, pp. 949–952, 2018.
- [8] P. Rungpichayapichet, M. Nagle, P. Yuwanbun, P. Khuwijitjaru, B. Mahayothee, and J. Müller, "Prediction mapping of physicochemical properties in mango by hyperspectral imaging," *Biosystems Eng.*, vol. 159, pp. 109–120, Jul. 2017.
- [9] S. Munera, C. Besada, N. Aleixos, P. Talens, A. Salvador, D.-W. Sun, S. Cubero, and J. Blasco, "Non-destructive assessment of the internal quality of intact persimmon using colour and VIS/NIR hyperspectral imaging," *LWT*, vol. 77, pp. 241–248, Apr. 2017.
- [10] T. Guo, M. Huang, Q. Zhu, Y. Guo, and J. Qin, "Hyperspectral image-based multi-feature integration for TVB-N measurement in pork," *J. Food Eng.*, vol. 218, pp. 61–68, Feb. 2018.
- [11] D. Tao, Z. R. Wang, G. L. Li, and L. Xie, "Sex determination of silkworm pupae using VIS-NIR hyperspectral imaging combined with chemometrics," *Spectrochimica Acta A, Mol. Biomol. Spectrosc.*, vol. 208, pp. 7–12, Feb. 2019.
- [12] D. Guo, Q. Zhu, M. Huang, Y. Guo, and J. Qin, "Model updating for the classification of different varieties of maize seeds from different years by hyperspectral imaging coupled with a pre-labeling method," *Comput. Electron. Agricult.*, vol. 142, pp. 1–8, Nov. 2017.
- [13] X. Zhang, "Interactive patent classification based on multi-classifier fusion and active learning," *Neurocomputing*, vol. 127, pp. 200–205, Mar. 2014.
- [14] M. Huang, J. Tang, B. Yang, and Q. Zhu, "Classification of maize seeds of different years based on hyperspectral imaging and model updating," *Comput. Electron. Agricult.*, vol. 122, pp. 139–145, Mar. 2016.
- [15] Y. LeCun, L. Bottou, Y. Bengio, and P. Haffner, "Gradient-based learning applied to document recognition," *Proc. IEEE*, vol. 86, no. 11, pp. 2278–2324, Nov. 1998.
- [16] A. Krizhevsky, I. Sutskever, and G. E. Hinton, "ImageNet classification with deep convolutional neural networks," in *Proc. NIPS*, vol. 25, 2012, pp. 1106–1114.
- [17] P. Sermanet, S. Chintala, and Y. LeCun, "Convolutional neural networks applied to house numbers digit classification," in *Proc. Int. Conf. Pattern Recognit. (ICPR)*, Nov. 2012, pp. 3288–3291.
- [18] K. Makantasis, K. Karantzalos, A. Doulamis, and N. Doulamis, "Deep supervised learning for hyperspectral data classification through convolutional neural networks," in *Proc. IEEE Int. Geosci. Remote Sens. Symp. (IGARSS)*, Jul. 2015, pp. 4959–4962.
- [19] J. Acquarelli, T. van Laarhoven, J. Gerretzen, T. N. Tran, L. M. C. Buydens, and E. Marchiori, "Convolutional neural networks for vibrational spectroscopic data analysis," *Analytica Chim. Acta*, vol. 954, pp. 22–31, Feb. 2017.
- [20] J. Liu, M. Osadchy, L. Ashton, M. Foster, C. J. Solomon, and S. J. Gibson, "Deep convolutional neural networks for Raman spectrum recognition: A unified solution," *Analyst*, vol. 142, no. 21, pp. 4067–4074, 2017.

- [21] A. Gummeson, I. Arvidsson, M. Ohlsson, N. C. Overgaard, A. Krzyzanowska, A. Heyden, A. Bjartell, and K. Åström, "Automatic Gleason grading of HE stained microscopic prostate images using deep convolutional neural networks," *SPIE Med. Imag.*, vol. 10140, Mar. 2017, Art. no. 101400S.
- [22] Y.-D. Zhang, K. Muhammad, and C. Tang, "Twelve-layer deep convolutional neural network with stochastic pooling for tea category classification on GPU platform," *Multimedia Tools Appl.*, vol. 77, no. 17, pp. 22821–22839, Sep. 2018.
- [23] R. G. Brereton and G. R. Lloyd, "Support Vector Machines for classification and regression," *Analyst*, vol. 135, no. 2, pp. 230–267, 2010.
- [24] J. Luts, F. Ojeda, R. Van de Plas, B. De Moor, S. Van Huffel, and J. A. Suykens, "A tutorial on support vector machine-based methods for classification problems in chemometrics," *Anal. Chim. Acta*, vol. 665, pp. 129–145, Apr. 2010.
- [25] M. P. Gómez-Carracedo, R. Fernández-Varela, D. Ballabio, and J. M. Andrade, "Screening oil spills by mid-IR spectroscopy and supervised pattern recognition techniques," *Chemometrics Intell. Lab. Syst.*, vol. 114, pp. 132–142, May 2012.
- [26] J. C. L. Alves and R. J. Poppi, "Determining the presence of naphthenic and vegetable oils in paraffin-based lubricant oils using near infrared spectroscopy and support vector machines," *Anal. Methods*, vol. 5, no. 22, pp. 6457–6464, 2013.
- [27] B.-C. Kuo, H.-H. Ho, C.-H. Li, C.-C. Hung, and J.-S. Taur, "A kernel-based feature selection method for SVM with RBF kernel for hyperspectral image classification," *IEEE J. Sel. Topics Appl. Earth Observ. Remote Sens.*, vol. 7, no. 1, pp. 317–326, Jan. 2014.
- [28] R. M. Balabin, R. Z. Safieva, and E. I. Lomakina, "Near-infrared (NIR) spectroscopy for motor oil classification: From discriminant analysis to support vector machines," *Microchem. J.*, vol. 98, no. 1, pp. 121–128, 2011.
- [29] M. Sokolova and G. Lapalme, "A systematic analysis of performance measures for classification tasks," *Inf. Process. Manag.*, vol. 45, no. 4, pp. 427–437, 2009.



DAN TAO received the Ph.D. degree in agricultural engineering from Southwest University, in 2019, where she is currently a Lectorate with East China Jiaotong University. Her research interests include machine learning, photoelectric information processing, and pattern recognition.



GUANGYING QIU received the M.S. degree in agricultural mechanical engineering from Southwest University, in 2017. He is currently a Laboratory Assistant with East China Jiaotong University. His research interests include deep learning, big data processing, and machine learning.



GUANGLIN LI received the Ph.D. degree in agricultural engineering from Southwest University, in 2002, where he is currently a Professor. His research interests include intelligent detection and control, image processing, and signal processing.

• • •